

Non-Fermi liquid behavior induced by inter-orbital scattering in hole-doped $\text{LiFe}_{1-x}\text{V}_x\text{As}$

L. Y. Xing,^{1,*} X. Shi,^{1,*} P. Richard,^{1,2,†} X. C. Wang,^{1,‡} Q. Q. Liu,¹ B. Q. Lv,¹ J.-Z. Ma,¹ B. B. Fu,¹ L.-Y. Kong,¹ H. Miao,³ T. Qian,¹ T. K. Kim,⁴ M. Hoesch,⁴ H. Ding,^{1,2,§} and C. Q. Jin^{1,2,¶}

¹*Beijing National Laboratory for Condensed Matter Physics,
and Institute of Physics, Chinese Academy of Sciences, Beijing 100190, China*

²*Collaborative Innovation Center of Quantum Matter, Beijing, China*

³*Condensed Matter Physics and Materials Science Department,
Brookhaven National Laboratory, Upton, New York 11973, USA*

⁴*Diamond Light Source, Harwell Campus, Didcot, OX11 0DE, United Kingdom*

(Dated: December 9, 2024)

We synthesized a series of V-doped $\text{LiFe}_{1-x}\text{V}_x\text{As}$ single crystals. The superconducting transition temperature T_c of LiFeAs decreases rapidly at a rate of 7 K per 1% V. The Hall coefficient of LiFeAs switches from negative to positive with 4.2% V doping, showing that V-doping introduces hole carriers. This observation is further confirmed by the evaluation of the Fermi surface volume measured by angle-resolved photoemission spectroscopy (ARPES), from which a 0.3 hole doping per V atom introduced is deduced. Interestingly, the introduction of holes does not follow a rigid band shift. We also show that the temperature evolution of the electrical resistivity as a function of doping indicates a crossover from a Fermi liquid to a non-Fermi liquid, and back again towards a Fermi liquid. Our ARPES data indicate that the non-Fermi liquid behavior is mostly enhanced when one of the hole d_{xz}/d_{yz} Fermi surfaces is well nested by the antiferromagnetic wave vector to the inner electron Fermi surface pocket with the d_{xy} orbital character. The magnetic susceptibility of $\text{LiFe}_{1-x}\text{V}_x\text{As}$ indicates that V acts as a strong magnetic impurity, thus providing a natural explanation to the rapid suppression of superconductivity upon V doping.

PACS numbers: 74.70.Xa, 74.25.F- , 74.25.Jb

The Fe-based superconductors are multi-band systems with a Fermi surface (FS) composed of several pockets with different orbital characters [1]. The complexity of the FS allows different low-energy scattering processes that can stabilize long-range magnetic order and that have even been proposed to induce superconducting pairing in these compounds [2–4]. A recent report on Co-doped LiFeAs revealed a direct correlation between FS nesting and manifestations of non-Fermi liquid behavior [5]. Indeed, the largest deviation of the temperature exponent in the power law used to fit the temperature dependence of the electrical resistivity is found for a doping corresponding to a good nesting of the largest hole FS pocket with d_{xy} character with the electron pockets. Unfortunately, whether the relevant scattering causing the non-Fermi liquid behavior is orbital-dependent is unclear. The most natural way to settle this issue is to hole-dope LiFeAs and search for similar scattering but with FS pockets carrying different orbital characters. Although attempts to dope the BaFe_2As_2 system with holes by substituting Fe by lighter $3d$ elements have been done using Mn [6–9] and Cr [10–14], literature lacks of similar study on the LiFeAs family, and in either cases V has not been used to induce hole doping.

In this Letter we report the synthesis and characterization of V-doped LiFeAs . The superconducting transition temperature T_c of LiFeAs is dramatically suppressed by V doping at a rate of 7 K per 1% V, which is much faster than for Co/Ni/Cu doping. Our Hall coefficient R_H and ARPES measurements indicate that each V dopant releases 0.3 hole carrier. With increasing the V-doping level, we observe a crossover from FL to Non-FL to FL behavior, which we explain by the increase of inter-orbital scattering mediated by low-energy spin fluctuations when a good nesting is found between the inner d_{xy} electron FS pocket at the M point and the outer d_{xz}/d_{yz} hole FS pocket at the Γ point. In addition, our susceptibility measurements suggest that V-doping gives rise to magnetic impurities, thus providing a simple explanation for the rapid suppression of T_c upon V doping.

The single crystals of $\text{LiFe}_{1-x}\text{V}_x\text{As}$ used in this study have been synthesized using the self-flux method and the details can be found elsewhere [15]. Li_3As and $\text{Fe}_{1-x}\text{V}_x\text{As}$ were first synthesized as precursors by a solid state reaction method. To synthesize Li_3As , Li lump and As powder were sealed into a Ti tube under 1 atm Ar and sintered at 650 °C for 10 hours. $\text{Fe}_{1-x}\text{V}_x\text{As}$ was obtained by mixing Fe, V and As powders, pressing into pieces and heating at 700 °C for 15 hours in an evacuated quartz tube. After the preparation of Li_3As , $\text{Fe}_{1-x}\text{V}_x\text{As}$ and As were mixed together according to $\text{Li}:\text{Fe}_{1-x}\text{V}_x\text{As}:\text{As}=1:0.3:1$, put into an alumina crucible, sealed into a Nb tube under 1 atm Ar atmosphere and sealed into a quartz tube. The mixture were first heated

* These authors contributed equally to this work

† p.richard@iphy.ac.cn

‡ wangxiancheng@iphy.ac.cn

§ dingh@iphy.ac.cn

¶ cqjin@iphy.ac.cn

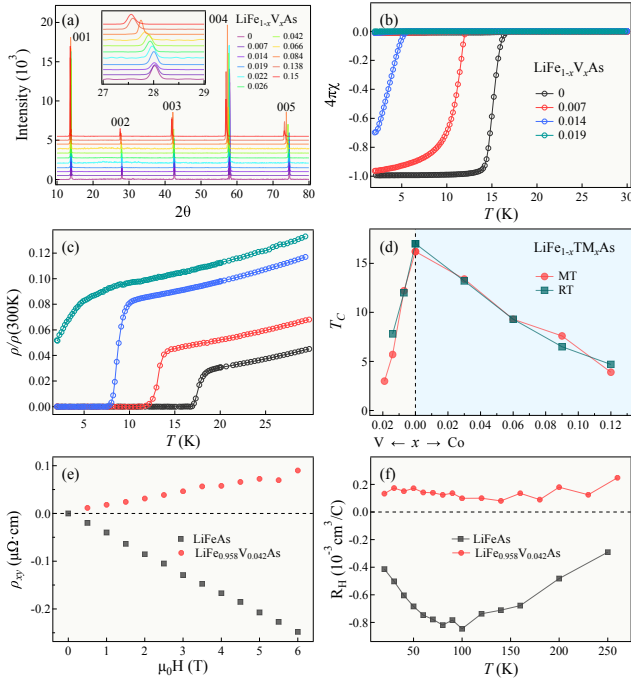


FIG. 1. (Color online) XRD patterns of $\text{LiFe}_{1-x}\text{V}_x\text{As}$ single crystals. (b) and (c) Temperature dependence of the magnetic susceptibility and the normalized resistivity $\rho/\rho(300\text{ K})$ of $\text{LiFe}_{1-x}\text{V}_x\text{As}$ single crystals. (d) Evolution of T_c as a function of V and Co doping in $\text{LiFe}_{1-x}\text{TM}_x\text{As}$ (TM = V and Co) single crystals. The data for $\text{LiFe}_{1-x}\text{Co}_x\text{As}$ are extracted from Ref. [15], copyright © (2014) by IOP Publishing. (e) Magnetic field dependence of the Hall resistivity ρ_{xy} of LiFeAs and $\text{LiFe}_{0.958}\text{V}_{0.042}\text{As}$ single crystals at 20 K. (f) Temperature dependence of the Hall coefficient R_H of LiFeAs and $\text{LiFe}_{0.958}\text{V}_{0.042}\text{As}$ single crystals.

to 1100 °C for 50 hours and then slowly cooled down to 750 °C at the rate of 2 °C/h to grow the single crystals.

Fig. 1(a) shows the x-ray diffraction (XRD) pattern of $\text{LiFe}_{1-x}\text{V}_x\text{As}$ single crystals. Only $00l$ peaks are observed and the full width at half maximum is smaller than 0.2° , which indicates the high quality of our single crystals. The inset is an enlarged view of the 002 peak, which moves towards lower 2θ with x increasing, indicating that the lattice parameter c increases with V doping. While superconductivity in most Fe-based superconductors occurs following carrier doping, a T_c of 18 K is observed in pristine LiFeAs [16, 17]. The T_c of LiFeAs decreases linearly upon electron doping with Co, Ni or Cu [15, 18]. Figs. 1(b) and 1(c) show the temperature dependence of the magnetic susceptibility and the resistivity for $\text{LiFe}_{1-x}\text{V}_x\text{As}$ with x smaller than 0.019. All $\text{LiFe}_{1-x}\text{V}_x\text{As}$ samples with $x < 0.019$ exhibit diamagnetic susceptibility and superconducting zero resistivity. The superconducting transition T_c decreases from 16 K to 6 K with x increasing to 0.014. Superconductivity disappears at $x = 0.019$, as shown in Fig.

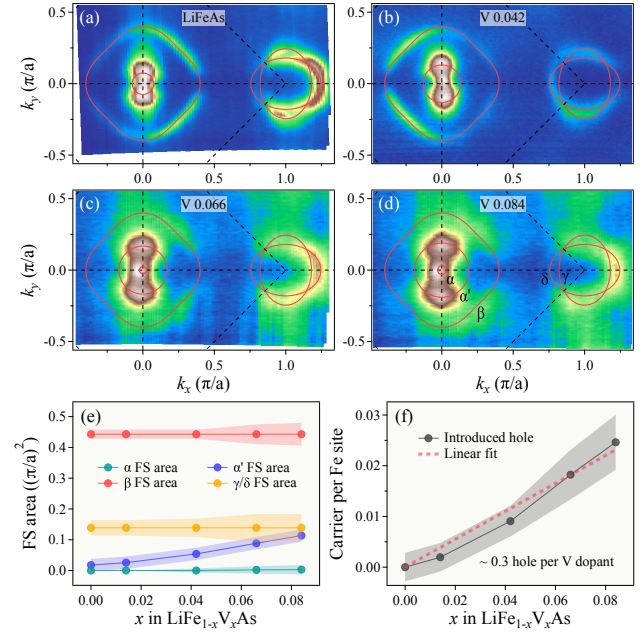


FIG. 2. (Color online) (a)-(d) ARPES FS intensity maps of $\text{LiFe}_{1-x}\text{V}_x\text{As}$ for $x = 0, 0.042, 0.066$ and 0.084 , respectively. The maps were recorded with s -polarized 51 eV photons and integrated within a 10 meV energy window centered at E_F . The red lines appended on the plots are extracted FS contours. (e) Calculated area of different FS pockets as a function of doping. (f) Number of carriers introduced by the $\text{Fe} \rightarrow \text{V}$ substitution deduced from the FS volume. The dashed pink line is a linear fit showing that 0.3 hole is added to the system for each V dopant.

1(c). As displayed in Fig. 1(d), T_c decreases almost linearly with V doping at a rate of 7 K per 1%V, which is a much faster suppression rate than for electron doping with Co/Ni/Cu [19, 20]. Indeed, 1% doping with Co and Ni in the $\text{LiFe}_{1-x}(\text{Co/Ni})_x\text{As}$ system suppresses T_c by 1 K and 2.2 K, respectively. Cu doping suppresses T_c at a rate similar to Ni doping but the FS almost does not change [15]. It was proposed that the suppression of T_c by Cu dopant is mainly due to its strong impurity scattering effect.

To further study the effect of V doping in the LiFeAs system, we conducted Hall resistivity measurements. Fig. 1(e) compares the Hall resistivity ρ_{xy} of LiFeAs and $\text{LiFe}_{0.958}\text{V}_{0.042}\text{As}$ versus applied magnetic field measured at 20 K. In contrast to LiFeAs , for which the slope of $d\rho_{xy}/dH$ is negative, the slope of $d\rho_{xy}/dH$ is positive for $\text{LiFe}_{0.958}\text{V}_{0.042}\text{As}$, suggesting that the substitution of Fe by V dopes the system with holes. The temperature dependence of the Hall coefficient R_H for these samples is shown in Fig. 1(f). For LiFeAs , R_H is negative with a minimum value at about 100 K, which is consistent with a previous work [21]. However, for the $\text{LiFe}_{0.958}\text{V}_{0.042}\text{As}$ sample, R_H is positive with a smaller temperature dependence within the measured temperature range. This

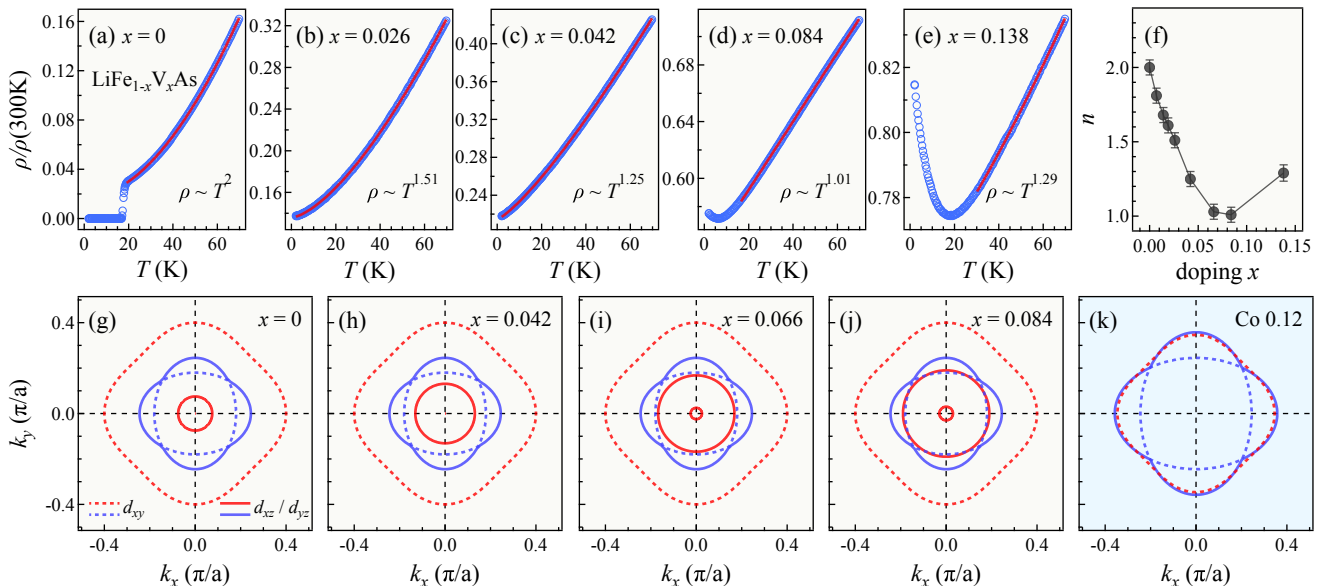


FIG. 3. (Color online) (a)-(e) Temperature dependence of the normalized resistivity $\rho/\rho(300\text{K})$ for five selected $\text{LiFe}_{1-x}\text{V}_x\text{As}$ single crystals. For each sample, $\rho/\rho(300\text{K})$ is fitted using $\rho = \rho_0 + AT^n$. (f) Exponent n as a function of x in $\text{LiFe}_{1-x}\text{V}_x\text{As}$. (g)-(j) Evolution of the hole FSs (red) and electron FSs (blue) as a function of x in $\text{LiFe}_{1-x}\text{V}_x\text{As}$. The electron FSs pockets have been shifted to the Γ point for a better comparison. (k) Same as (g)-(j) but for $\text{LiFe}_{0.88}\text{Co}_{0.12}\text{As}$ (extracted from Ref. [5]), which shows the most pronounced non-Fermi liquid behavior in the $\text{LiFe}_{1-x}\text{Co}_x\text{As}$ series.

reversal sign of R_H is an explicit indication of hole doping with the introduction of V.

In order to confirm and quantify the introduction of hole carriers in the V-doped LiFeAs samples, we also performed ARPES measurements at the Dreamline beamline of Shanghai Synchrotron Radiation Facility and at the I05 beamline of Diamond Light Source using a Scienta D80 analyzer and a Scienta R4000 analyzer, respectively. The energy and angular resolutions have been set to 10 meV and 0.2° , respectively. All measurements have been recorded at 20 K with 51 eV photons ($k_z \approx 0$ [22]) in a s polarization configuration. We show in Figs. 2(a)-2(d) the FS measured for the V doping levels $x = 0, 0.042, 0.066$ and 0.084 , respectively. For each sample, hole FS pockets at Γ and electron FS pockets at M are observed, as indicated by the red contours extracted from the ARPES intensity maps. The FS topology is typical of that of most iron-pnictides [1]. According to the Luttinger theorem, the electronic carrier concentration is determined by the algebraic sum of all the FS areas. The calculated area of each FS pocket as a function of doping is shown in Fig. 2(e), and the deduced hole carrier concentration is illustrated in Fig. 2(f). As expected, the substitution of Fe by V leads to hole doping. However, by applying a simple linear fit to the introduced free carrier concentration as a function of the V content, we conclude that only 0.3 hole carrier is introduced per substituting V dopant. This doping is ten times smaller than the “nominal” one, which contrasts with the Co and

Ni-doped cases [5, 18]. Co-doping into LiFeAs can be approximated by a rigid band shift with one free electron introduced for each Co atom. The electron FS pockets become larger while the hole FS pockets shrink upon Co-doping in LiFeAs, with their algebraic sum respecting the Luttinger theorem [5]. The situation is quite different in V-doped LiFeAs. As indicated in Fig. 2(e), the change in the free carrier concentration is practically related only to the α' FS pocket, thus indicating that V-doping does not follow a rigid band shift.

A recent report on Co-doped LiFeAs indicates that the improvement upon doping of the nesting conditions between the hole and electron FS pockets leads to a Fermi liquid to non-Fermi liquid behavior [5]. As the size of the α' FS pocket increases with V-doping, whereas the electron FS pockets remain nearly unchanged, one can wonder if FS nesting can also lead to a non-Fermi liquid in this system. To check this scenario, we measured the resistivity of the $\text{LiFe}_{1-x}\text{V}_x\text{As}$ samples and fitted the data with $\rho = \rho_0 + AT^n$, as shown in Fig. 3. The doping evolution of the exponent n is displayed in Fig 3(f). As with Co-doped LiFeAs, the exponent n deviates from 2 with the introduction of V dopants, suggesting a non-Fermi liquid regime. Interestingly, n reaches a minimum of 1.07 for a doping of $x = 0.084$, before increasing again towards 2 with doping further the system. This behavior strongly suggests that V-doped LiFeAs is also host to low-energy fluctuations enhanced with the nesting conditions. As shown, in Fig. 3(j), a good nesting is found

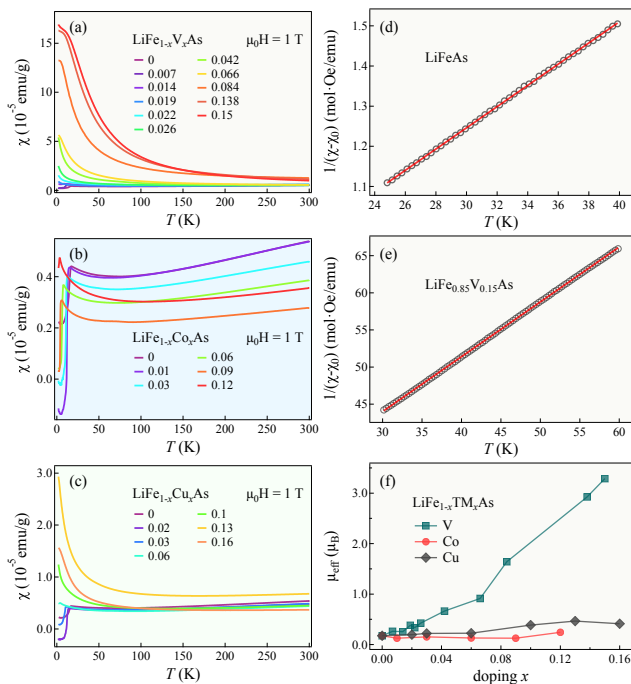


FIG. 4. (Color online) Temperature dependence of the magnetic susceptibility in a 1 T magnetic field of (a) $\text{LiFe}_{1-x}\text{V}_x\text{As}$, (b) $\text{LiFe}_{1-x}\text{Co}_x\text{As}$ and (c) $\text{LiFe}_{1-x}\text{Cu}_x\text{As}$ single crystals. (d) and (e) Magnetic susceptibility fitted according to the Curie-Weiss law $1/(\chi - \chi_0) = (T - \theta)/C$. (f) Effective moment as a function of the doping concentration x for $\text{LiFe}_{1-x}\text{TM}_x\text{As}$ (TM = V, Co and Cu) single crystals.

at $x = 0.084$ between the α' FS pocket, which carries a d_{xz}/d_{yz} orbital character, and the inner electron FS pocket (γ), which mainly derives from the d_{xy} orbital. This situation is symmetrical to the one found in Co-doped LiFeAs , for which the lowest n coincides to the best nesting conditions between the outer hole FS pocket (β) with a d_{xy} orbital character and the outer electron FS pocket (δ), which carries a dominant d_{xz}/d_{yz} orbital character [Fig. 3(k)]. Consequently, it is fair to say that non-Fermi liquid behavior is mainly due to low-energy inter-orbital scattering with the scattering vector \mathbf{Q} corresponding to the wavevector between Γ and M. Such experimental observation is consistent with theoretical calculations indicating that the coupling to the wave vector \mathbf{Q} is favored between different orbital states [23].

However, our data suggest that the magnetic properties of $\text{LiFe}_{1-x}\text{V}_x\text{As}$ go beyond simple FS nesting. When x exceeds 0.066, $\text{LiFe}_{1-x}\text{V}_x\text{As}$ starts displaying a semiconducting behavior at low temperature similar to the one observed in Cu-doped Fe-based superconductors. Indeed, a weak semiconducting behavior emerges at $x \sim 0.13$ for $\text{LiFe}_{1-x}\text{Cu}_x\text{As}$ [24] and at $x \sim 0.033$ for $\text{NaFe}_{1-x}\text{Cu}_x\text{As}$ [20]. A crossover from metallic to

semiconducting behavior with Cu doping has also been observed in $\text{BaFe}_{1-x}\text{Cu}_x\text{As}$ [25], $\text{SrFe}_{1-x}\text{Cu}_x\text{As}$ [26] and $\text{Fe}_{1.01-x}\text{Cu}_x\text{Se}$ [27], and it was proposed that Cu dopants in these materials behave like strong scatterers inducing a metal-insulator transition due to the Anderson localization mechanism [28]. Since the critical doping for the metal-semiconductor crossover is even lower in $\text{LiFe}_{1-x}\text{V}_x\text{As}$, *i.e.* $x = 0.066$ in $\text{LiFe}_{1-x}\text{V}_x\text{As}$ as compared with $x = 0.4$ in $\text{LiFe}_{1-x}\text{Co}_x\text{As}$ and $x = 0.13$ in $\text{LiFe}_{1-x}\text{Cu}_x\text{As}$, we also assume that the V impurities are strong scattering centers.

In order to determine whether the V dopants are magnetic or not, we measured the magnetic susceptibility under magnetic field up to 1 T. The amplitude of the magnetic susceptibility in $\text{LiFe}_{1-x}\text{V}_x\text{As}$ [Fig. 4(a)] is about one order of magnitude higher than for $\text{LiFe}_{1-x}\text{Co}_x\text{As}$ [Fig. 4(b)] and $\text{LiFe}_{1-x}\text{Cu}_x\text{As}$ [Fig. 4(c)]. As shown in Figs. 4(d) and 4(e), respectively, the susceptibilities of LiFeAs and $\text{LiFe}_{0.85}\text{V}_{0.15}\text{As}$ follow the Curie-Weiss law $1/(\chi - \chi_0) = (T - \theta)/C$ at low temperature, where θ is the Curie temperature. The Curie-Weiss law allows us to extract an effective magnetic moment μ_{eff} . The results as a function of the substitution content, displayed in Fig. 4(f), indicate that while the effective magnetic moment varies only slightly upon Co and Cu doping, it is greatly enhanced with V doping. This suggests the formation of magnetic V impurity in $\text{LiFe}_{1-x}\text{V}_x\text{As}$, which is similar to Mn dopants in $\text{Na}(\text{Fe}_{0.97-x}\text{Co}_{0.03}\text{Mn}_x)\text{As}$ [29] and differs from the weakly magnetic Co and Cu impurities in $\text{LiFe}_{1-x}\text{Co}_x\text{As}$ and $\text{LiFe}_{1-x}\text{Cu}_x\text{As}$. The observation of strong magnetic V impurities offers a natural explanation to the rapid suppression of T_c in $\text{LiFe}_{1-x}\text{V}_x\text{As}$.

In summary, we synthesized and characterized single crystals of $\text{LiFe}_{1-x}\text{V}_x\text{As}$. Using Hall coefficient and ARPES measurements, we showed that the substitution of Fe by V dopes the system with holes at a rate of 0.3 hole/V. We showed from the temperature dependence of the resistivity data that the system exhibits a non-Fermi liquid behavior that is enhanced around doping where our ARPES measurements indicate a good FS nesting between FS pockets carrying different orbital characters, suggesting that the non-Fermi liquid behavior is induced by low-energy inter-orbital scattering by the antiferromagnetic wave vector. Finally, the magnetic susceptibility of $\text{LiFe}_{1-x}\text{V}_x\text{As}$ shows that V acts as a strong, magnetic scattering center, thus providing a natural explanation for the rapid suppression of superconductivity found upon doping.

We acknowledge Jiang-Ping Hu for useful discussions. This work was supported by grants from MOST (2011CBA001000, 2011CBA00102, 2012CB821403, 2013CB921700 and 2015CB921301) and NSFC (11004232, 11034011/A0402, 11234014, 11274362, 11474330 and 11474344) of China. We acknowledge Diamond Light Source for time on beamline I05 under proposal SI11452.

-
- [1] P. Richard, T. Sato, K. Nakayama, T. Takahashi and H. Ding, *Rep. Prog. Phys.* **74**, 124512 (2011).
- [2] I. I. Mazin, D. J. Singh, M. D. Johannes and M. H. Du, *Phys. Rev. Lett.* **101**, 057003 (2008).
- [3] H. Ding, P. Richard, K. Nakayama, K. Sugawara, T. Arakane, Y. Sekiba, A. Takayama, S. Souma, T. Sato, T. Takahashi, Z. Wang, X. Dai, Z. Fang, G. F. Chen, J. L. Luo and N. L. Wang, *Europhys. Lett.* **83**, 47001 (2008).
- [4] S. Graser, T. A. Maier, P. J. Hirschfeld and D. J. Scalapino, *N. J. Phys.* **11**, 025016 (2009).
- [5] Y. M. Dai, H. Miao, L. Y. Xing, X. C. Wang, P. S. Wang, H. Xiao, T. Qian, P. Richard, X. G. Qiu, W. Yu, C. Q. Jin, Z. Wang, P. D. Johnson, C. C. Homes and H. Ding, *Phys. Rev. X* **5**, 031035 (2015).
- [6] Y. Liu, D. L. Sun, J. T. Park, C. T. Lin, *Physica C* **470**, S513 (2010).
- [7] M. G. Kim, A. Kreyssig, A. Thaler, D. K. Pratt, W. Tian, J. L. Zarestky, M. A. Green, S. L. Bud'ko, P. C. Canfield, R. J. McQueeney and A. I. Goldman, *Phys. Rev. B* **82**, 220503(R) (2010).
- [8] A. Thaler, H. Hodovanets, M. S. Torikachvili, S. Ran, A. Kracher, W. Straszheim, J. Q. Yan, E. Mun and P. C. Canfield, *Phys. Rev. B* **84**, 144528 (2011).
- [9] A. Pandey, V. K. Anand and D. C. Johnston, *Phys. Rev. B* **84**, 014405 (2011).
- [10] A. S. Sefat, D. J. Singh, L. H. VanBebber, Y. Mozharivskyj, M. A. McGuire, R. Jin, B. C. Sales, V. Keppens and D. Mandrus, *Phys. Rev. B* **79**, 224524 (2009).
- [11] S. L. Bud'ko, S. Nandi, N. Ni, A. Thaler, A. Kreyssig, A. Kracher, J.-Q. Yan, A. I. Goldman, and P. C. Canfield, *Phys. Rev. B* **80**, 014522 (2009).
- [12] E. Colombier, M. S. Torikachvili, N. Ni, A. Thaler, S. L. Bud'ko and P. C. Canfield, *Supercond. Sci. Technol.* **23**, 054003 (2010).
- [13] K. Marty, A. D. Christianson, C. H. Wang, M. Matsuda, H. Cao, L. H. VanBebber, J. L. Zarestky, D. J. Singh, A. S. Sefat and M. D. Lumsden, *Phys. Rev. B* **83**, 060509(R) (2011).
- [14] J. P. Clancy, B. D. Gaulin and A. S. Sefat, *Phys. Rev. B* **85**, 054115 (2012).
- [15] L. Y. Xing, H. Miao, X. C. Wang, J. Ma, Q. Q. Liu, Z. Deng, H. Ding and C. Q. Jin, *J. Phys.: Condens. Matter* **26**, 435703 (2014).
- [16] X. C. Wang, Q. Q. Liu, Y. X. Lv, W. B. Gao, L. X. Yang, R. C. Yu, F. Y. Li and C. Q. Jin, *Solid Stat. Commun.* **148**, 538 (2008).
- [17] J. H. Tapp, Z. Tang, B. Lv, K. Sasmal, B. Lorenz, P. C. W. Chu and A. M. Guloy, *Phys. Rev. B* **78**, 060505(R) (2008).
- [18] M. J. Pitcher, T. Lancaster, J. D. Wright, I. Franke, A. J. Steele, P. J. Baker, F. L. Pratt, W. T. Thomas, D. R. Parker, S. J. Blundell and S. J. Clarke, *J. Am. Chem. Soc.* **132**, 10467 (2010).
- [19] P. C. Canfield, S. L. Bud'ko, N. Ni, J. Q. Yan and A. Kracher, *Phys. Rev. B* **80**, 060501 (2009).
- [20] A. F. Wang, J. J. Lin, P. Cheng, G. J. Ye, F. Chen, J. Q. Ma, X. F. Lu, B. Lei, X. G. Luo and X. H. Chen, *Phys. Rev. B* **88**, 094516 (2013).
- [21] O. Heyer, T. Lorenz, V.B. Zabolotnyy, D.V. Evtushinsky, S.V. Borisenko, I. Morozov, L. Harnagea, S. Wurmehl, C. Hess and B. Büchner, *Phys. Rev. B* **84**, 064512 (2011).
- [22] H. Miao, T. Qian, X. Shi, P. Richard, T.K. Kim, M. Hoesch, L.Y. Xing, X.-C. Wang, C.-Q. Jin, J.-P. Hu and H. Ding, *Nat. Commun.* **6**, 6056 (2015).
- [23] J. Zhang, R. Sknepnek, R. M. Fernandes and J. Schmalian, *Phys. Rev. B* **79**, 220502(R) (2009).
- [24] L. Y. Xing, X. C. Wang, Z. Deng, S. J. Zhang, S. M. Feng, W. M. Li, Q. Q. Liu and C. Q. Jin, *Int. J. Mod. Phys. B* **29**, 1542023 (2015).
- [25] N. Ni, A. Thaler, J. Q. Yan, A. Kracher, E. Colombier, S. L. Bud'ko, P. C. Canfield and S. T. Hannahs, *Phys. Rev. B* **82**, 024519 (2010).
- [26] Y. J. Yan, P. Cheng, J. J. Ying, X. G. Luo, F. Chen, H. Y. Zou, A. F. Wang, G. J. Ye, Z. J. Xiang, J. Q. Ma and X. H. Chen, *Phys. Rev. B* **87**, 075105 (2013).
- [27] A. J. Williams, T. M. McQueen, V. Ksenofontov, C. Felser and R. J. Cava, *J. Phys.: Condens. Matter* **21**, 305701 (2009).
- [28] S. Chadov, D. Schärf, G. H. Fecher, C. Felser, L. Zhang and D. J. Singh, *Phys. Rev. B* **81**, 104523 (2010).
- [29] Q. Deng, X. Ding, S. Li, J. Tao, H. Yang and H.-H. Wen, *New J. Phys.* **16**, 063020 (2014).